This document was prepared in conjunction with work accomplished under Contract No. DE-AC09-96SR18500 with the U. S. Department of Energy.

DISCLAIMER

PEAK STRIPPING METHODOLOGY FOR PLUTONIUM ANALYSIS IN THE PRESENCE OF NEPTUNIUM

Chris Hodge
Westinghouse Savannah River Company
Aiken, SC, 29803, USA

Abstract

Quantitative Plutonium analysis depends upon the accurate identification of the assay peak. The Np[Pa] equilibrium pair introduces interfering peaks in ^{239}Pu, ^{238}Pu, and ^{235}U assay peak region. When an interfering peak is present, it negates the assay unless an appropriate technique can be developed to deal with the interference. Peak Stripping is one such technique. Peak stripping involves an algorithm to strip an entire peak from another, resulting in a spectrum that can then be analyzed for the isotope of interest. A simpler method is a 'pseudo-peak-stripping" whereby the effects of the interfering peak are quantified and those effects are stripped from the assay data. In this case the integrated peak areas are analyzed and corrected.

There are two methods presented in this paper. Both assimilate the integrated data for the assay peak regions (in this case ^{238}Pu, ^{239}Pu, and ^{235}U) and for the Neptunium/Protactinium secular equilibrium pair ([Np[Pa]). Using Np[Pa] assumes that the Protactinium has come to equilibrium with Neptunium. This requires only ~ 6months from the time chemical purification. Therefore it is a valid assumption in most cases. A correction is then applied to the assay peak areas to "strip" the underlying effects of Np[Pa].

Introduction

Quantitative Plutonium analysis depends upon the accurate identification of the assay peak. When an interfering peak is present, it negates the assay unless an appropriate technique can be developed to deal with the interference. Peak Stripping is one such technique. Peak stripping involves an algorithm to strip an entire peak from another, resulting in a spectrum that can then be analyzed for the isotope of interest. A simpler method is a 'pseudo-peak-stripping" whereby the effects of the

interfering peak are quantified and those effects are stripped from the assay data. In this case the integrated peak areas are analyzed and corrected.

Two methods are presented in this paper. Both assimilate the integrated data for the assay peak regions (in this case ^{238}Pu, ^{239}Pu, and ^{235}U) and for the Neptunium/Protactinium secular equilibrium pair ([Np[Pa]). Both calculate a stripping factor normalized relative to the Np[Pa] 312 keV peak. Using Np[Pa] assumes that the Protactinium has come to equilibrium with Neptunium. This requires only ~ 6 months from the time of chemical separation, therefore, it is a valid assumption in most cases. A correction is then applied to the assay peak areas to "strip" the underlying effects of Np[Pa].

The analytical model, based on 1st principles of physics, uses known branching ratios and specific activities to calculate theoretical peak intensities from Np[Pa] that might interfere with SNM assay peaks. This method calculates the detector efficiency (ε) curve based on the major Np[Pa] peaks.

The empirical model is an experimental method based solely on measuring the Np[Pa] interfering peaks and ratioing those intensities to the Np[Pa] 312 keV peak. It is not necessary to determine ε as it is intrinsic in the methodology.

Pu and Np[Pa] γ-ray Spectroscopy

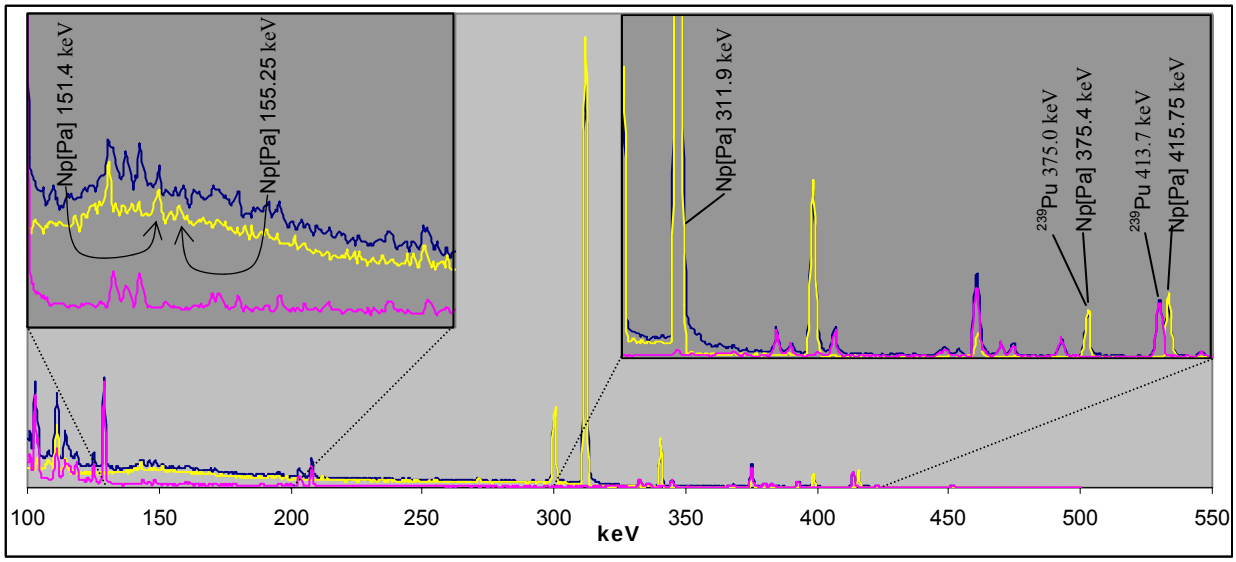

Figure 1 – Typical ^{239}Pu and Np[Pa] Spectra

Figure 1 presents gamma spectra of typical ^{239}Pu and Np[Pa] standards: 1 gram Np[Pa] in yellow, 10 grams ^{239}Pu in magenta, and the two assayed together in blue. Expanded scales are inlayed for the 130-200 (upper-left) and 300-425 (upper-right) keV regions of the same spectra to better demonstrate details. An interesting observation is that the intensity of the 415.75 keV peak for 1 gram of Np[Pa] is approximately the same as the intensity of the 413.7 keV peak for 10 grams of ^{239}Pu.

The Np[Pa] 311.9 keV is Np[Pa]'s most abundant peak and there are no known significant interferences from SNM isotopes. Therefore, it is the reference peak used to quantify the SNM assay peak interferences from Np[Pa].

The figure also points out ^{239}Pu's primary assay peak @ 413.7 keV and Np[Pa]'s interfering peak @ 415.75 keV. This paper will use ^{239}Pu's 414 keV peak to demonstrate the presented techniques. These same techniques can be applied to the other stripping factors as well. In Figure 1, it appears as if ^{239}Pu's 414 peak and Np[Pa]'s 416 peak are resolvable and they are for multiple gram quantities as shown. Our typical measurements are of much smaller quantities (>>0.1 gram) and the data is normally attenuated by gloveboxes, containers, and other materials yielding a significantly less resolved spectrum. Typical peak resolution is ~3keV. Anything less assumes too much about the effects of gain (energy) stability, geometry, attenuating materials, deadtime, and distance. Therefore, assay peak regions are normally set broadly at ~411 to 418keV to fully encompass both the 414 from ^{239}Pu and the 416 from Np[Pa].

Additionally, Figure 1 highlights two other regions of interest: the 153 keV (^{238}Pu) and the 375 keV (secondary peak of ^{239}Pu) regions. These are the other two regions with significant interferences from Np[Pa]. Note the small relativity intensity in the 153 keV region.

Specific Np[Pa], and Pu, and U data

The following equations are used in the algorithms described in this paper:

$$\check{R}\ [\gamma/s]/g = SA_i * BR_{i,j} * k_{Ci} * \varepsilon_{detector,\ j}$$

Equation 1 – Ř, γ-Ray Count Rate

where: SA_i = Specific Activity of isotope$_i$
$BR_{i,j}$ = Branching Ratio of peak$_j$ for isotope$_i$
k_{Ci} = 3.70E+10 d/Ci

assuming: $\varepsilon_{detector,\ j}$ = 1 (detector efficiency @ energy$_j$)

$A_{Pa} = A_{Np}$ @ secular equilibrium (after ~6 months)

$$A_{Pa} = SA_{Np}\ N_{Np}$$

Equation 2 – Activity

where: A = activity
N = number of atoms

Table 1 presents pertinent data used in the development of these stripping algorithms. In some cases, where more than one interfering peaks exists (i.e. beyond the resolving capabilities for the field mode this detector setup), the contributions are summed, denoted by a "**}**" symbol. Ř represents the number of γ-rays produced at a specific energy from 1 gram of a specific isotope. Since the Np[Pa] 312 keV peak is used as the normalization peak, the significance of each individual peak was compared to it. It is not statistically significant to attempt to correct for peaks with significance ($\check{R}_i/\ \check{R}_{312}$) much less than 1%. Literature values for branching ratios were also compared and are discussed in a subsequent

section. BR^1 and BR^2 are branching ratios from different literature sources. The percent difference ($\Delta BR_{1,2}$) between the two is also presented to demonstrate the error introduced from literature values.

isotope	SA ci/g	peak keV	BR^1 (%) γ/d	Ř (ε=1) [γ/s]/g		affected assay peak	significance γ_i/γ_{312}	BR^2 (%) γ/d	$\Delta BR_{1,2}$ (%)
^{238}Pu	17	152.7	0.00127	7.99E+06			91%	0.000937	26%
		766.35	0.000031	1.95E+05			2%	0.000022	29%
^{239}Pu	6.19E-02	129.3	0.0062	1.42E+05			2%	0.00631	-2%
		311.69	0.000027	6.18E+02	} 6.64E+02	312	0.007%		
		313.5	0.0000020	4.58E+01			0.0005%		
		375.0	0.00158	3.62E+04			0.41%	0.001554	2%
		413.7	0.00151	3.46E+04			0.39%	0.001466	3%
^{235}U	2.16E-06	185.7	54	4.32E+04			0.49%	57.2	-6%
^{237}Np	7.04E-04	29.4	9.8	2.55E+06			29%	15	-53%
		111.5	0.35	9.12E+04			1%	0.0026	99%
		131.11	0.112	2.92E+04	} **5.42E+04**	129	0.617%	0.085	24%
		134.28	0.096	2.50E+04				0.067	30%
		151.41	0.263	6.85E+04	} **9.59E+04**	153	1.092%	0.232	12%
		155.25	0.105	2.74E+04				0.092	12%
		184.4	0.011	2.87E+03	} **4.17E+03**	186	0.047%	0.02	-82%
		187	0.005	1.30E+03				0.003	40%
^{233}Pa	2.05E+04	98.44	15.5	4.04E+06			46%		
		111	5.28	1.38E+06			16%		
		300.11	5.8	1.51E+06			17%	6.62	-14%
		311.9	33.7	**8.78E+06**			100%	38.6	-15%
		340.47	3.88	1.01E+06			12%	4.47	-15%
		375.4	0.59	**1.54E+05**		375	1.8%	0.679	-15%
		398.5	1.29	**3.36E+05**			3.8%	1.39	-8%
		415.75	1.59	**4.14E+05**		414	4.7%	1.745	-10%
^{241}Am	3.42E+00	310.3	0.000015	1.90E+04	} **1.83E+05**	312	0.2%		
		311.94	0.00013	1.65E+05			1.9%		

Table 1 – Specific Spectroscopy for ^{238}Pu, ^{239}Pu, ^{235}U, ^{241}Am, ^{233}Pa, and ^{237}Np.

[1] NuclideNavigator™ V3.4, June 2000

[2] http://georg.pnpi.spb.ru/russian/gammas/

Analytical Model Based on First Principles

The Analytical model is based upon Ř as presented in Table 1. The model calculates the ratio of Řs relative to the Np[Pa] 312 keV normalization peak. Therefore, with the analytical model, the Np[Pa] 312 peak is measured and multiplied by the pseudo ε ($\mathcal{P}\varepsilon_i$) derived for assay peak$_i$. This product is representative of the interference in peak$_i$ due to Np[Pa] and can be directly stripped (subtracted) from the measured assay peak$_i$ resulting in the net assay peak$_i$.

The data in Table 1 assumes detector efficiency (ε) of 1 even though ε_i is never exactly equal to 1. However, for a model based upon ratios of Ř, the ratio of $\varepsilon_i / \varepsilon_{INp[Pa]\ 312}$ is all that is required and simplifies matters. For energies greater than 312keV (i>312), $\varepsilon_i / \varepsilon_{Np[Pa]\ 312}$ can be assumed to be 1. For energies less than 312keV, ε_i needs to be determined. This can be accomplished by measuring known Np[Pa] γ-rays of energies less than 312keV and determining an equation that fits the observed $\varepsilon_i / \varepsilon_{Np[Pa]\ 312}$.

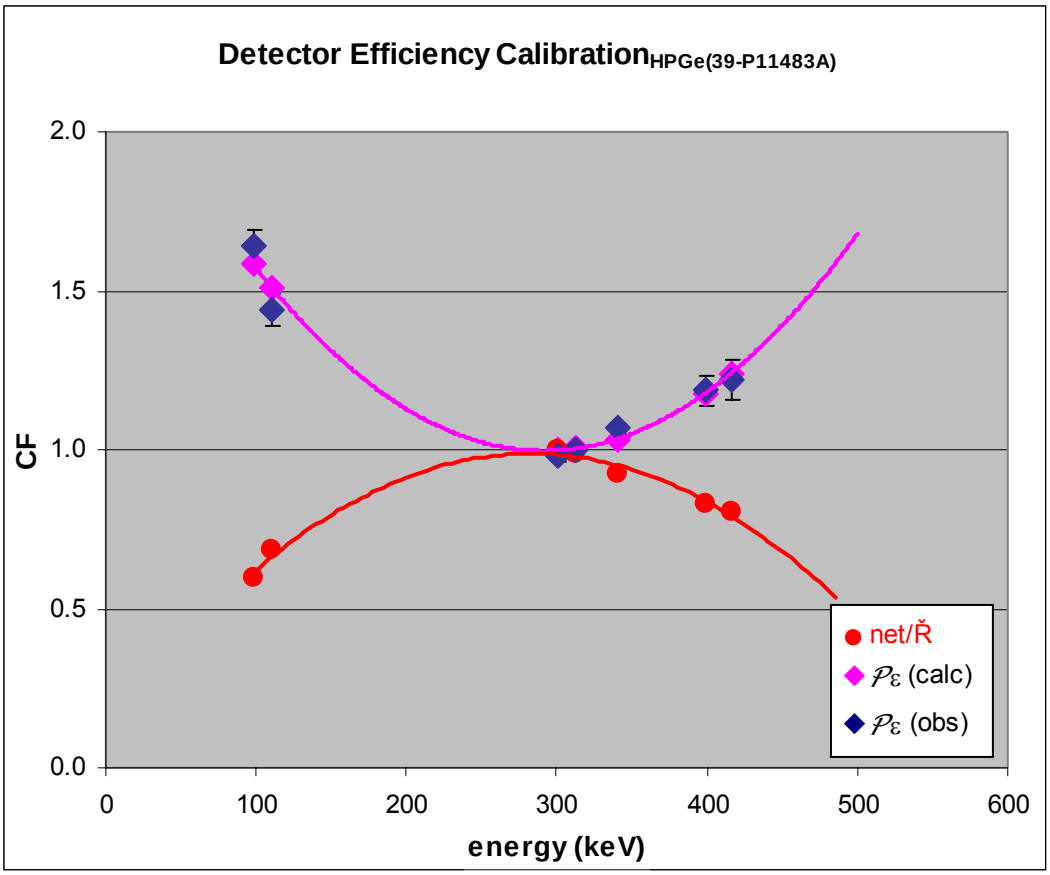

Figure 2 – Detector Efficiency Calibration and Resulting Pseudo Efficiency ($\mathcal{P}\varepsilon$) Factor Analysis

Figure ***2*** displays the empirical data and the results from such a calculation. The normalized empirical data (net$_i$/Ř$_i$) from the Np[Pa] data is represented by the red dots. The blue triangles, along with associated 2σ uncertainties error bars, are the derived values of $\mathcal{P}\varepsilon_i$ from this empirical data.

Performing a regression analysis on this data yields the magenta curve defined by Equation 3.

$$\mathcal{P}\varepsilon_{calc} = 0.0053\ e^{-700E} + 1$$

Equation 3 – $\mathcal{P}\varepsilon_{calc}$, Calculated Pseudo Efficiency Factor

Where $\mathcal{P}\varepsilon$ are the calculated $\varepsilon_i/\varepsilon_{INp[Pa]\ 312}$ as represented by the magenta triangles.

The data correlates well within the observed 2σ. The calculated $\mathcal{P}\varepsilon$s show how this can be corrected. Since the model is all normalized to Np[Pa] 312, $\varepsilon_{detector,\ i}$ can now be determined with Equation 3 and substituted into Equation 1.

Table 2 presents the empirical data collected to calculated ε. There were fifteen spectra acquired over various assay times, distances, and quantities of Np[Pa]. Data collection criteria such as time, distance and even quantity are considered in a relational calculation such as the one described herein. When data is normalized by one peak within a spectrum, all data collection details cancel out. This is a clean way to compile the data as it cancels out much of the empirical error.

energy				
98	**111**	**300**	**312**	**340**
4.77E+6	1.94E+6	2.96E+6	1.72E+7	1.85E+6
4.78E+6	1.96E+6	3.02E+6	1.71E+7	1.84E+6
4.77E+6	1.95E+6	2.99E+6	1.72E+7	1.86E+6
4.71E+6	1.98E+6	2.97E+6	1.71E+7	1.84E+6
4.72E+6	1.97E+6	2.93E+6	1.68E+7	1.81E+6
2.88E+6	1.19E+6	1.77E+6	1.02E+7	1.09E+6
2.88E+6	1.19E+6	1.80E+6	1.02E+7	1.09E+6
2.87E+6	1.19E+6	1.82E+6	1.02E+7	1.11E+6
2.89E+6	1.20E+6	1.76E+6	1.01E+7	1.09E+6
2.88E+6	1.20E+6	1.77E+6	1.02E+7	1.11E+6
9.18E+5	3.78E+5	5.85E+5	3.35E+6	3.63E+5
9.13E+5	3.77E+5	5.98E+5	3.33E+6	3.62E+5
9.55E+5	4.00E+5	5.90E+5	3.35E+6	3.56E+5
9.42E+5	3.92E+5	5.82E+5	3.36E+6	3.61E+5
9.23E+5	3.87E+5	5.75E+5	3.34E+6	3.63E+5

Table 2 – Np[Pa] data (Ř) corrected for Compton and Ambient Background

Table 3 completes the calculation with the normalization of the data (by the Np[Pa]312 peak), calculating averages and errors. BR^1 data was added for ease of understanding the calculations.

$$\mathcal{P}\varepsilon_{obs} = BR^1/\text{average}$$

Equation 4 – $\mathcal{P}\varepsilon_{obs}$, Observed Pseudo Efficiency Factor

$\mathcal{P}\varepsilon_{calc}$ is calculated by Equation 3. Table 3 provides the tabular results plotted in Figure 2 and Figure 3.

	energy				
	98.4	111	300	312	340
$\frac{peak_i}{peak_{312}}$	0.27732	0.11305	0.17215	1.00000	0.10756
	0.27922	0.11468	0.17654	1.00000	0.10718
	0.27810	0.11382	0.17438	1.00000	0.10809
	0.27542	0.11571	0.17381	1.00000	0.10752
	0.28079	0.11695	0.17426	1.00000	0.10787
	0.28233	0.11714	0.17387	1.00000	0.10718
	0.28231	0.11695	0.17627	1.00000	0.10717
	0.28055	0.11606	0.17844	1.00000	0.10897
	0.28554	0.11901	0.17388	1.00000	0.10818
	0.28341	0.11776	0.17435	1.00000	0.10874
	0.27396	0.11275	0.17463	1.00000	0.10844
	0.27379	0.11316	0.17917	1.00000	0.10860
	0.28512	0.11958	0.17617	1.00000	0.10633
	0.28066	0.11685	0.17330	1.00000	0.10747
	0.27654	0.11610	0.17218	1.00000	0.10879
average x BR	9.42	3.91	5.89	33.70	3.64
σ_{rel}	1.3%	1.8%	1.2%	0.0%	0.7%
BR[1]	15.50	5.63	5.80	33.70	3.88
$\mathcal{P}\varepsilon_{obs}$	1.64	1.44	0.98	1.00	1.07
$2\sigma_{abs}$	0.044	0.053	0.023	0.000	0.015
ε_i $(1/\mathcal{P}\varepsilon_{obs})$	*0.608*	*0.694*	*1.016*	*1.000*	*0.937*
$\mathcal{P}\varepsilon_{calc}$	1.58	1.51	1.00	1.00	1.03

Table 3 – Table 2 Normalized by the Np[Pa] 312 peak and Reduced Calculations

Figure 3 demonstrates the success of this method. It presents the typical detector efficiency curve for a HPGe detector[3] in green and the calculated efficiency (ε_i) based on Equation 3 for Np[Pa]'s five most abundant peaks in magenta.

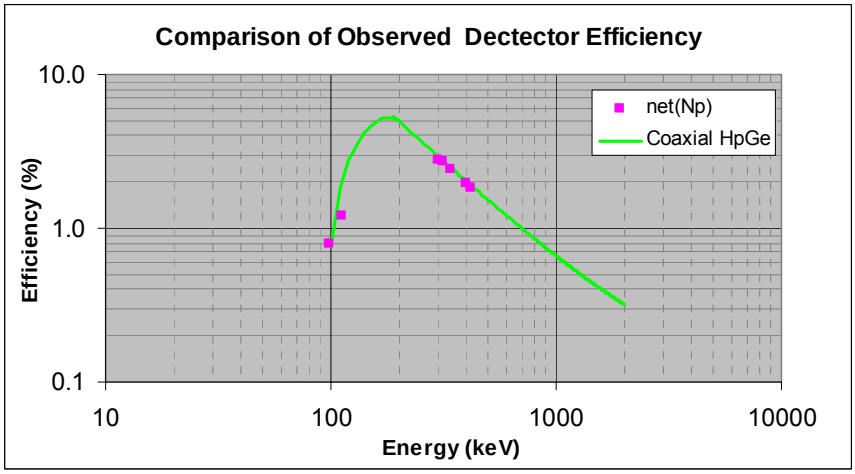

Figure 3 – Comparison of Observed Detector Efficiency with Manufacturer's Specifications

[3] Germanium Detector User's Manual, Canberra Industries part # 9231358A, (1998).

Table 4 presents the individual errors for each collected data point. The errors are well within acceptable limits and further demonstrate the effectiveness of Equation 3.

energy				
98.4	**111**	**300**	**312**	**340**
5%	-2%	0%	0%	4%
4%	-3%	-2%	0%	4%
5%	-3%	-1%	0%	3%
6%	-4%	-1%	0%	4%
4%	-5%	-1%	0%	3%
3%	-5%	-1%	0%	4%
3%	-5%	-2%	0%	4%
4%	-5%	-3%	0%	2%
2%	-7%	-1%	0%	3%
3%	-6%	-1%	0%	2%
6%	-2%	-1%	0%	3%
6%	-2%	-4%	0%	3%
2%	-7%	-2%	0%	5%
4%	-5%	0%	0%	4%
5%	-5%	0%	0%	2%

Table 4 – Tabulated Errors for Calculated $\mathcal{P}\varepsilon_i$

Table 5 shows the calculated $\mathcal{P}\varepsilon$s for the assay energy peaks, the calculated rate ($\check{R}$) at ε =1, and the errors for each data point. $\check{R}_{peak}/\check{R}_{312}$ is the ratio of the assay peak region relative to the 312 keV. It is interesting to note the relative abundances. This ratio will become significant in the conclusion when discussion data quality and significance.

isotope	Pu^{239}	Pu^{238}	U^{235}	$Np[Pa^{233}]$	Pu^{239}	Pu^{239}
energy	129	153	186	312	375	414
$\mathcal{P}_\varepsilon$	1.41	1.30	1.17	1.00	1.11	1.23
$\check{R}$ (ε=1)	5.42E+04	9.6E+4	4.2E+3	8.8E+6	1.5E+5	4.1E+5
$\check{R}_{peak}/\check{R}_{312}$	0.62%	1.09%	0.05%	100.00%	1.75%	4.72%
	-230%	-18%	-177%	0%	6%	-2%
	-213%	37%	-701%	0%	7%	-2%
	-222%	-2%	-127%	0%	7%	0%
	-214%	20%	-170%	0%	3%	-2%
	-190%	20%	-25%	0%	7%	-1%
	-173%	23%	-149%	0%	3%	0%
calc-obs	-230%	-7%	-1720%	0%	4%	-2%
obs	-208%	-29%	-120%	0%	7%	0%
	-205%	-16%	-146%	0%	8%	-2%
	-267%	-17%	-155%	0%	0%	0%
	-147%	-6%	-129%	0%	7%	1%
	-367%	-46%	-57%	0%	9%	-3%
	-178%	-23%	88%	0%	9%	6%
	-189%	-23%	-110%	0%	0%	-6%
	1851%	31%	-133%	0%	14%	-2%

Table 5 – Δ(%) Between Observed and Calculated Data in the Assay Peak Regions

Table 6 presents the final conclusion for the analytical model. These are the factors and associated errors that would be used to "strip" Np[Pa] interferences from SNM assay peaks.

isotope	Pu^{239}	Pu^{238}	U^{235}	Pu^{239}	Pu^{239}
energy	129	153	186	375	414
$SF_{1st\ princ}$	4.37E-03	8.41E-03	4.05E-04	1.58E-02	3.83E-02
$\sigma_{1st\ princ}$	17.9%	18.1%	17.9%	17.8%	18.2%

Table 6 – Np[Pa] Interference Stripping Factors Based on 1st Principles

The real test of the method is the calculation of the errors associated with interferences of the assay peaks. The "assay peak" is actually the associated interference from Np[Pa], that is the Np[Pa] peak that would interfere with the given assay peak. As one can observe from Table 5 once the method is applied to the assay peaks, the results are not as satisfactory as they were for the Np[Pa] calculations. This is most noticeable for the low energy ^{238}Pu 153 keV peak. The count rates and resulting statistics are much lower leading to higher errors. The Np[Pa] regions associated with the ^{239}Pu 129 keV and ^{235}U 186 keV are statistically insignificant and therefore also have very large associated errors. This will be further addressed in the conclusion section.

Empirical Model

The same data was analyzed strictly as an empirical correction. That is, first principles were not applied, a calculation was simply performed to equate the total gammas in the assay peak region to that found in the Np[Pa] 312 keV region. Table 7 gives the raw data and Table 8 the Np[Pa] 312keV normalized data (all rates divided by the associated 312 keV peak rate). The negative values in the table were presented to demonstrate the lack of statistical quality for the 129 keV and 186 keV regions. The data for these regions is statistically insignificant and represent no significant interference with assay peaks.

Pu^{239} 129	Pu^{238} 153	U^{235} 186	Np^{237} 312	Pu^{239} 375	Pu^{239} 414
-5.80E+4	1.76E+5	-9.08E+3	1.72E+7	2.56E+5	6.72E+5
-6.63E+4	1.05E+5	-1.15E+3	1.71E+7	2.54E+5	6.68E+5
-6.13E+4	1.47E+5	-2.56E+4	1.72E+7	2.53E+5	6.56E+5
-6.56E+4	1.20E+5	-9.85E+3	1.71E+7	2.62E+5	6.66E+5
-8.16E+4	1.18E+5	9.05E+3	1.68E+7	2.50E+5	6.50E+5
-6.08E+4	7.00E+4	-8.41E+3	1.02E+7	1.57E+5	3.90E+5
-3.42E+4	9.24E+4	-2.55E+2	1.02E+7	1.56E+5	3.96E+5
-4.14E+4	1.20E+5	-2.11E+4	1.02E+7	1.52E+5	3.91E+5
-4.23E+4	1.02E+5	-8.98E+3	1.01E+7	1.48E+5	3.95E+5
-2.66E+4	1.03E+5	-7.44E+3	1.02E+7	1.61E+5	3.88E+5
-3.13E+4	3.00E+4	-4.75E+3	3.35E+6	4.95E+4	1.27E+5
-5.45E+3	5.17E+4	3.17E+3	3.33E+6	4.83E+4	1.32E+5
-1.89E+4	3.66E+4	7.21E+2	3.35E+6	4.87E+4	1.21E+5
-1.65E+4	3.66E+4	-1.37E+4	3.36E+6	5.31E+4	1.36E+5
7.48E+2	2.14E+4	-4.07E+3	3.34E+6	4.62E+4	1.31E+5

Table 7 – Assay Peak Count Rates Corrected for Compton and Ambient Backgrounds

Table 8 also provides the average and associated error for each peak, a reminder of the literature branching ratios (BR^1), the normalized literature branching ratios(BR_{312}/BR_x), the relative observed branching ratios(BR_{ref}/BR_{obs}), calculated branching ratios utilizing a non-linear least squares fit of the data (calc BR_{ref}/BR_{obs}), the relative error between the observed and calculated branching ratios (Δ%). The relative observed branching ratios(BR_{ref}/BR_{obs}) vary as expected with energy.

The calculated branching ratios were calculated utilizing a non-linear least squares fit of the data (calc BR_{ref}/BR_{obs}). Ideally, these all should equal unity. The relative error between the observed and calculated branching ratios (Δ%) is a reflection of poor statistics and deviations in reported branching ratios.

Isotope	Pu^{239}	Pu^{238}	U^{235}	Np^{237}	Pu^{239}	Pu^{239}
energy	129	153	186	312	375	414
$\frac{peak_i}{peak_{312}}$	-297	98	-1893	1	67	26
	-258	163	-14833	1	67	26
	-280	117	-671	1	68	26
	-261	143	-1734	1	65	26
	-206	142	1859	1	67	26
	-168	146	-1213	1	65	26
	-298	110	-39977	1	65	26
	-247	85	-485	1	67	26
	-239	100	-1127	1	68	26
	-382	99	-1366	1	63	26
	-107	112	-705	1	68	26
	-611	64	1052	1	69	25
	-177	91	4645	1	69	28
	-203	92	-245	1	63	25
	4460	156	-820	1	72	26
Average	48.4	114.5	-3834.2	1.0	67.0	25.9
σ	2535.1%	25.3%	-282.0%	0.0%	3.5%	2.5%
BR^1	5.42E+04	9.59E+04	4.17E+03	8.78E+06	1.54E+05	4.14E+05
BR_{312}/BR_x	162.0	91.6	2106.3	1.0	57.1	21.2
BR_{ref}/BR_{obs}	335%	80%	-55%	100%	85%	82%
calc BR_{ref}/BR_{obs}	-0.196	-0.197	-0.198	-0.201	-0.203	-0.204
Δ%	105.8%	124.6%	64.0%	120.1%	123.8%	125.0%

Table 8 – Table 7 Normalized by the Np[Pa] 312 keV Peak and Reduced Calculations.

Table 9 presents the conclusion of this section, the SFs for Np[Pa] interferences of SNM assay peaks for the empirical model.

Isotope	Pu^{239}	Pu^{238}	U^{235}	Np^{237}	Pu^{239}	Pu^{239}
energy	129	153	186	312	375	414
SF	**4.46E-3**	**9.13E-3**	**3.51E-4**	**1.00E+0**	**1.47E-2**	**3.89E-2**
σ	33.9%	25.3%	407.7%	0.0%	4.1%	2.5%

Table 9 – Np[Pa] Interference Stripping Factors Based on the Empirical Model

As before, the real test is an examination of the error associated with each data point once this model is applied. Table 10 provides the individual relative errors between calculated branching ratios and observed (Table 8 provides the averages for each energy). As before, the relative high abundance peaks (375 and 414 keV regions) do well and low abundance peaks yield large errors. As expected, the ^{238}Pu 153 errors are higher that the ^{239}Pu region, but still statistically significant.

Pu^{239} 129	Pu^{238} 153	U^{235} 186	Np^{237} 312	Pu^{239} 375	Pu^{239} 414
713.2%	14.7%	50.6%	0.0%	-0.2%	1.1%
634.2%	-42.3%	-286.9%	0.0%	-0.5%	0.9%
678.9%	-2.0%	82.5%	0.0%	-1.2%	-1.1%
638.8%	-24.6%	54.8%	0.0%	2.6%	0.9%
526.2%	-24.4%	148.5%	0.0%	-0.5%	0.0%
446.9%	-27.2%	68.4%	0.0%	2.9%	-1.1%
716.1%	3.7%	-942.7%	0.0%	2.3%	0.6%
610.6%	25.8%	87.4%	0.0%	-0.6%	-1.0%
594.2%	13.0%	70.6%	0.0%	-2.1%	1.1%
890.9%	13.4%	64.4%	0.0%	6.0%	-1.3%
321.4%	2.3%	81.6%	0.0%	-1.1%	-2.0%
1364.4%	43.7%	127.4%	0.0%	-3.0%	2.5%
466.4%	20.1%	221.1%	0.0%	-2.6%	-6.8%
520.8%	19.8%	93.6%	0.0%	5.6%	4.8%
-9123.0%	-36.0%	78.6%	0.0%	-7.8%	1.2%

Table 10 – Calculated Percent Errors of Interference Peaks Based on the Empirical Model

Conclusion

Isotope	Pu^{239}	Pu^{238}	U^{235}	Pu^{239}	Pu^{239}
energy	129	153	186	375	414
$SF_{1st\ princ}$	4.37E-03	**8.41E-3**	4.05E-04	**1.58E-2**	**3.83E-2**
$\sigma_{1st\ princ}$	17.9%	18.1%	17.9%	17.8%	18.2%
$SF_{empirical}$	4.46E-3	**8.74E-3**	-2.61E-4	**1.49E-2**	**3.86E-2**
$\sigma_{empirical}$	33.9%	25.3%	-282.0%	3.5%	2.5%
Δ(%) SF_{emp}/SF_{1st}	2%	4%	255%	-6%	1%
average net/MLD	-0.55	1.11	-0.24	18.24	63.55

Table 11 – Empirical Stripping Factors

Table 11 summarizes the results derived from both models. There is excellent agreement and the results are statistically identical.

As previously demonstrated (Figure 1, Table 1, Table 5, Table 8, and Table 10), the Np[Pa] data in the ^{239}Pu 129 keV and ^{235}U 186 keV are not statistically significant. Further evidence for this is pointed out in Table 11 with the ratio of average net counts to the observed Minimum Level of Detection (MLD). For both regions, MLD is much greater than the data in the associated peaks. Therefore, this report recommends that effects of Np[Pa] not be stripped from these regions. That is, these regions are statistically free from the effects of Np[Pa].

The factors presented for ^{239}Pu 375 keV and ^{239}Pu 414 keV are statistically sound with low associated errors. The effects of Np[Pa] can readily and accurately be stripped from these regions. The ^{238}Pu 153 keV SF is marginal as denoted by the larger error, small net/MLD ratio, and counting statistics as Figure 1 demonstrates so graphically. However, with the understanding of the larger associated error, this report recommends the stripping of Np[Pa] effects from the ^{238}Pu 153 keV region as well.